4-15-2015

A Full-Wave Model For a Binary Gas Thermosphere: Effects of Thermal Conductivity and Viscosity

Michael P. Hickey Ph.D.
Embry-Riddle Aeronautical University, hicke0b5@erau.edu

R. L. Walterscheid
Space Science Applications Laboratory; The Aerospace Corporation

G. Schubert
Department of Earth, Planetary, and Space Sciences; University of California

AGU PUBLICATIONS

JGR

Journal of Geophysical Research: Space Physics

RESEARCH ARTICLE
10.1002/2014JA020583

Key Points:
- Molecular dissipation impacts species fluctuations in a binary gas thermosphere
- O leads N_2 density fluctuations with molecular dissipation and mutual diffusion

Correspondence to:
M. P. Hickey,
michael.hickey@erau.edu

Citation:
Hickey, M. P., R. L. Walterscheid, and G. Schubert (2015), A full-wave model for a binary gas thermosphere: Effects of thermal conductivity and viscosity, *J. Geophys. Res. Space Physics*, *120*, 3074–3083, doi:10.1002/2014JA020583.

Received 4 SEP 2014
Accepted 6 MAR 2015
Accepted article online 11 MAR 2015
Published online 15 APR 2015

A full-wave model for a binary gas thermosphere: Effects of thermal conductivity and viscosity

M. P. Hickey[1], R. L. Walterscheid[2], and G. Schubert[2,3]

[1]Department of Physical Sciences, Embry-Riddle Aeronautical University, Daytona Beach, Florida, USA, [2]Space Science Applications Laboratory, The Aerospace Corporation, Los Angeles, California, USA, [3]Department of Earth, Planetary, and Space Sciences, University of California, Los Angeles, California, USA

Abstract The thermosphere is diffusively separated and behaves as a multiconstituent gas wherein individual species in static equilibrium are each stratified according to their individual scale heights. Gravity waves propagating in the thermosphere cause individual gases to oscillate with different amplitudes and phases. We use a two-gas (N_2 and O) full-wave model to examine the roles of thermal conductivity, viscosity, and mutual diffusion on the wave-induced characteristics of both gases. In the lower thermosphere, where the gases are relatively tightly coupled, the major gas (N_2) controls the minor gas (O) response. At higher altitudes, the gases become thermally and inertially decoupled, and the wave in each constituent propagates and dissipates consistent with a dispersion relation and vertical scale determined from the constituent scale height. The effects of coupling and diffusion on the relative phases and amplitudes of the fluctuations in each gas are significantly altered by viscosity and thermal conductivity.

1. Introduction

Wave motion (primarily vertical) in a diffusively separated atmosphere with height-dependent composition drives the atmosphere out of diffusive equilibrium and causes fluctuations in each constituent to oscillate out of phase and with different fractional density amplitudes [*Del Genio*, 1978; *Del Genio et al.*, 1978, 1979a, 1979b]. *Innis and Conde* [2002] have inferred fractional density amplitudes and phases of O and N_2 in gravity waves propagating in the upper thermosphere at high geomagnetic latitudes using data obtained by the Neutral Atmosphere Composition Spectrometer and the Wind and Temperature Spectrometer instruments on Dynamics Explorer 2. They found general agreement between the observations and theoretical predictions of *Del Genio et al.* [1979a, 1979b]. Wave-like variations in nitrogen and oxygen density data from the Neutral Atmosphere Temperature Instrument on Atmospheric Explorer C have also been found to be consistent with predictions of gravity wave propagation in a multicomponent thermosphere [*Gross et al.*, 1984].

Density fluctuations that have been previously observed can be explained by considering the two competing terms in the continuity equation for each gas, as explained by *Del Genio et al.* [1979a]. The vertical advection term leads to a density increase over the positive half cycle of the wave, as denser air from below is advected upward. Simultaneously, the adiabatic expansion accompanying the upward vertical motion contributes to a density decrease. The latter effect is represented by the velocity divergence term in the continuity equation, and is the same for each species when their velocities are approximately equal, and occurs at low thermospheric heights where collisions between species are frequent. The former (advection) effect depends on the distribution of each species with height (expressed by the individual species scale heights) and so is larger for the heavier species of shorter-scale height. For the heaver gas, advection dominates over expansion, leading to a large positive response compared to the lighter gas. A light gas having a very large scale height may experience a negative response (reduction in density) out of phase with the heavier gas in this positive cycle of the wave.

The theory of *Del Genio et al.* [1979a, 1979b] accounts for the effects of height-dependent coupling and mutual diffusion on gravity wave-driven fluctuations of different species comprising a two-component thermosphere. However, it does not account for the effects of molecular viscosity and thermal conductivity. *Walterscheid and Hickey* [2012] generalized the equations of *Del Genio* [1978] and *Del Genio et al.* [1978, 1979a, 1979b] for wave propagation in a binary gas to include the effects of molecular diffusion of heat and momentum. Their model also accounts for the collisional transfer of heat and momentum between the two constituents. They used the model to evaluate the ability of one-gas models to approximate the binary model and found

that a one-gas model that conserves mean molecular weight provides a reasonable approximation. Here we use the binary model of *Walterscheid and Hickey* [2012] to evaluate the effects of viscosity and thermal conductivity on the wave-induced properties of both gases. We will show that viscous dissipation and thermal conduction, which cause a diffusion of momentum and heat, respectively, significantly modify wave amplitudes and phases obtained when only mutual diffusion is operative.

2. Theory, Model, and Basic State

The binary gas full-wave model that we describe here is based upon our single-gas full-wave model described by *Hickey et al.* [1997].

The linearized equations for one component of a two-constituent atmosphere, including the effects of wave-induced diffusion, heat and momentum transfer via collisional coupling with the other species, and molecular and eddy diffusion of heat and momentum, are given by *Del Genio* [1978] and *Walterscheid and Hickey* [2012]

$$\frac{\partial n_s'}{\partial t} + \overline{n}_s \underline{\nabla} \cdot \underline{v}_s' + w_s' \frac{d\overline{n}_s}{dz} = 0 \tag{1}$$

$$m_s \overline{n}_s \frac{\partial \underline{v}_s'}{\partial t} + \underline{\nabla} p_s' - m_s n_s' \underline{g} + 2 m_s \overline{n}_s \underline{\Omega}_f x \underline{v}_s' + r_s \underline{\nabla} \cdot \underline{\underline{\sigma}}_s' - \underline{\nabla} \cdot \left(m_s \overline{n}_s \eta_e \underline{\nabla} v_s' \right) = K_{st} \left(\underline{v}_t' - \underline{v}_s' \right) + m_s \overline{n}_s \nu_{nsi} \left(\underline{v}_i' - \underline{v}_s' \right) \tag{2}$$

$$c_{vs} \overline{n}_s m_s \frac{\partial T_s'}{\partial t} + \overline{p}_s \underline{\nabla} \cdot \underline{v}_s' + \underline{\underline{\sigma}}_s' : \underline{\nabla} \underline{v}_s' - r_s \underline{\nabla} \cdot \left(\kappa_{ms} \underline{\nabla} T_s' \right) - \frac{c_{ps} \overline{T}}{\overline{\theta}} \underline{\nabla} \cdot \left(\overline{n}_s \overline{m}_s \kappa_e \underline{\nabla} \theta_s' \right) = \frac{3k}{m_s + m_t} K_{st} \left(T_t' - T_s' \right) \tag{3}$$

$$\frac{p_s'}{\overline{p}_s} = \frac{n_s'}{\overline{n}_s} + \frac{T_s'}{\overline{T}_s} \tag{4}$$

The equations are, respectively, the linearized equations of (1) mass continuity, (2) momentum conservation, (3) energy conservation, and (4) the ideal gas equation of state. The subscripts s and t refer to the two atmospheric constituents. An identical set of equations (with s and t everywhere interchanged) applies to the species t. Here n is the number density, $\underline{v}'$ is the fluid perturbation velocity with vertical component w', p is the partial pressure, T is the temperature, m is the molecular mass, k is the Boltzmann's constant, $\underline{g}$ is the gravitational acceleration, and K_{st} is the collisional parameter describing the efficiency of momentum and heat exchange between the two gases. Also, κ_{ms} is the coefficient of molecular thermal conductivity, κ_e is the coefficient of eddy diffusivity, ν_{ni} is the neutral-ion collision frequency, $\underline{v}_i'$ is the ion perturbation velocity, and r_s is a coefficient that depends on the number density mixing ratio of species s, as described further below. The quantity θ is the potential temperature, given by $T(p_{00}/p)^{R/c_p}$, where R is the gas constant, c_p is the specific heat at constant pressure, and p_{00} is a reference pressure. An overbar denotes the basic undisturbed state (defined by the Mass Spectrometer Incoherent Scatter (MSIS) model [*Hedin*, 1991]), and primes denote deviations from that state. The viscous stress tensor appearing in equations (2) and (3) is given by

$$\left(\sigma_{ij} \right)_s' = \mu_s \left\{ \frac{\partial \left(v_i' \right)_s}{\partial x_j} + \frac{\partial \left(v_j' \right)_s}{\partial x_i} - \frac{2}{3} \delta_{ij} \underline{\nabla} \cdot \underline{v}_s' \right\} \tag{5}$$

where μ is the coefficient of molecular viscosity and δ_{ij} is the Kronecker delta. The coefficient r_s that multiplies the viscous and thermal conduction terms in equations (2) and (3) is equal to the number density mixing ratio for species $s (r_s = n_s/(n_s + n_t))$. This ensures that the effect of constituent t on shortening the mean free path of constituent s and thereby diminishing its viscosity is included [*Walterscheid and Hickey*, 2012]. The formula for μ_s is

$$\mu_s = \frac{M_s \overline{c}_s}{3\pi d_s^2} \tag{6}$$

where M is the molecular weight, $\overline{c}$ is the mean particle speed, and d is the molecular diameter [*Walterscheid and Hickey*, 2012].

The assumptions of hard elastic spheres and a Maxwellian velocity distribution for each species result in the following expression for the coupling coefficient K_{st} [*Burgers*, 1969; *Schunk*, 1977; *Del Genio*, 1978]

$$K_{st} = \frac{8}{3}\sigma^2 \overline{n}_s \overline{n}_t \left(\frac{2\pi m_s m_t k \overline{T}}{m_s + m_t}\right)^{1/2} \tag{7}$$

where σ is the sum of the radii of the colliding spheres. Division of K_{st} by the basic state mass density $m_s n_s$ gives a collision frequency, where the subscript s on K_{st} refers to the gas to which the prognostic equation for momentum or heat applies.

The two constituents are allowed to have different temperature perturbations and to exchange heat with each other [*Del Genio*, 1978]. The exchange of momentum between the two species is also included. In contrast to *Del Genio* [1978], we include the eddy and molecular diffusion of heat and momentum. In the present simulations, we neglect the Coriolis force and the ion drag in order to focus our attention on the viscous and thermal damping of the wave.

To solve equations (1) to (4), they are first linearized. A monochromatic, steady state wave solution is assumed having the form $\exp i(\omega t - kx)$, where ω and k (both real) are the angular frequency and horizontal wave number in the x direction, respectively. Substitution of this solution into the set of equations (1) to (4) yields a set of coupled, second-order differential equations in the vertical coordinate. These equations are numerically integrated from the lower to the upper boundary using the tridiagonal algorithm described by *Bruce et al.* [1953] and *Lindzen and Kuo* [1969]. The lower boundary is set well below the region of interest, and a sponge layer is implemented [e.g., *Hickey et al.*, 2000]. We employ a lower sponge layer with the lower boundary placed 450 km below the ground. This prevents multiple reflections at the ground and the buildup of trapped waves when the direct wave is of primary interest. The wave forcing is through the addition in the energy equation of an inhomogeneous heat source term of narrow vertical extent applied at an altitude $z = 80$ km. The N_2 forcing is a factor $\left(\overline{\rho}\,\overline{c}_p\right)_{N_2} / \left(\overline{\rho}\,\overline{c}_p\right)_O$ greater than the O forcing, which leads to an initially equal temperature response for each species.

At the upper boundary (650 km altitude), a radiation condition is imposed using a dispersion equation that includes dissipation [*Hickey and Cole*, 1987]. A sponge layer is also implemented to absorb any waves reflected from the upper boundary. The sponge layers are described by the following

$$K_R(z) = \Omega_L \exp((z_L - z)/H_L) + \Omega_U \exp((z - z_U)/H_U) \tag{8}$$

Here $\Omega = \omega - \underline{k} \cdot \underline{U}$ is the wave intrinsic frequency, where ω is the wave extrinsic frequency, $\underline{k}$ is the wave number vector, and $\underline{U}$ is the mean horizontal wind vector. Also, z_L and H_L are, respectively, the altitude and characteristic decay height associated with the lower sponge, while the upper sponge is similarly defined with subscript "u." Equation (8) defines the coefficient of Rayleigh friction. The identical form is also used to define the coefficient of Newtonian cooling.

We consider both isothermal and nonisothermal basic state atmospheres. The isothermal case allows for analytic solutions and by comparison with the nonisothermal case allows an assessment of temperature gradient effects. In the isothermal case, the temperature is 634 K, the average of the MSIS-90 temperatures at 120 km (368 K) and 500 km altitude [*Hedin*, 1991]. This gives reasonable values of density over the altitude region of interest. In the nonisothermal case, temperature is given by the MSIS-90 model at altitudes above 120 km, with a mean exospheric temperature of 900 K. At lower altitudes, the temperature is forced to become isothermal, smoothly decreasing to a value of 240 K below about 90 km altitude. We make the lower atmospheric region isothermal in order to preclude wave reflection that could be associated with structure in the lower atmosphere mean state, thus allowing us to isolate physical effects that originate solely in the thermosphere. Altitude profiles of temperature in the isothermal and nonisothermal cases are shown in Figure 1a.

The two constituents in our binary gas model are N_2 and O. Their basic state densities are set to the MSIS values at 120 km altitude, $n_s(120)$.With the pressure at 120 km altitude as a reference, the pressures at other altitudes are obtained by assuming diffusive equilibrium and integrating the barometric equation using the local scale height values for N_2 and O ($H_s = RT/M_s g$ is the scale height of constituent s, and M_s is its atomic or molecular weight). The mass density and number density are then calculated using the ideal gas equation

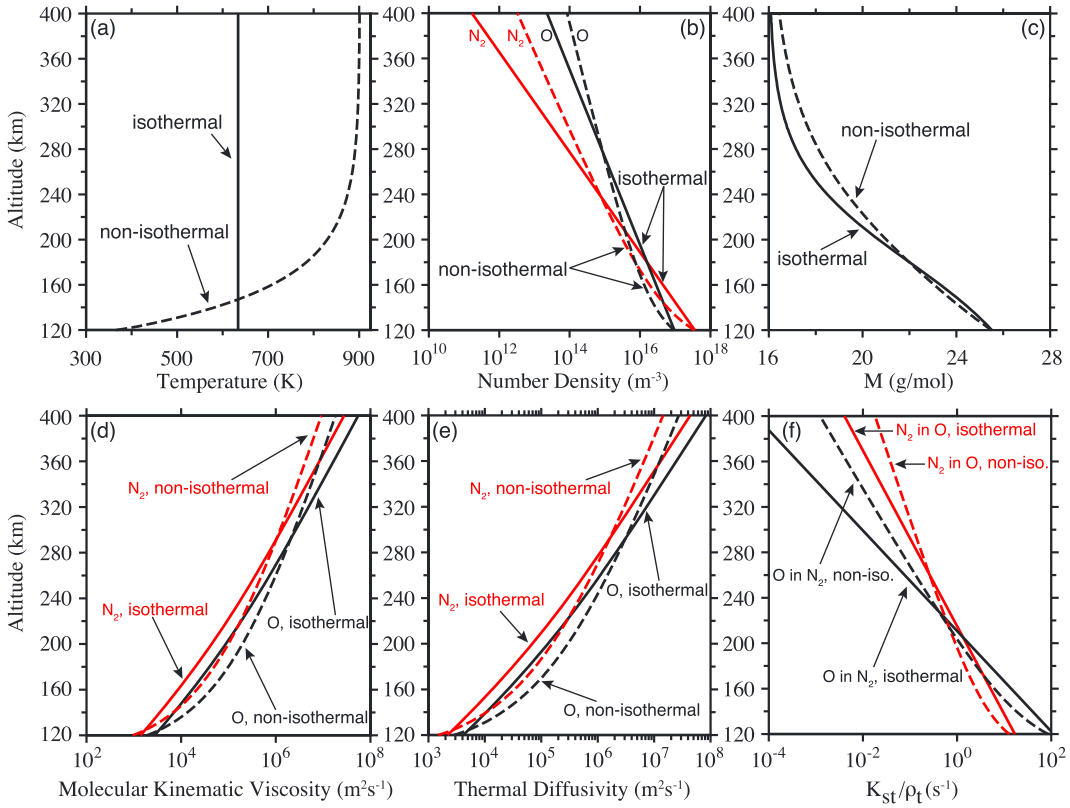

Figure 1. Basic state (a) temperature, (b) number densities, (c) molecular weight, (d) effective molecular kinematic viscosity, (e) effective thermal diffusivity, and (f) collision frequency for the isothermal and nonisothermal atmosphere.

of state for N_2 and O. This simplification of the basic state follows that of *Del Genio et al.* [1978, 1979a]. It was employed to facilitate comparison with *Del Genio et al.* [1979a, 1979b] and is consistent with our focus on wave propagation and multiconstituent effects above 120 km altitude. The altitude profiles of the basic state number densities of N_2 and O are shown in Figure 1b. The variation of molecular weight with altitude in this binary gas basic state is shown in Figure 1c. Figures 1d and 1e show the variation with height of the effective molecular kinematic viscosity $(r_s\mu_s/\overline{\rho}_s)$ and effective thermal conductivity $(r_s\kappa_{ms}/\overline{\rho}_s c_{vs})$, respectively, of each species in the basic state. Figures 1a–1e consider both the isothermal and nonisothermal states.

Low in the atmosphere where the collision frequency is high, the two species, s and t, will have the same velocity $\left(\underline{v}_s^{'} = \underline{v}_t^{'}\right)$ and temperature $\left(T_s^{'} = T_t^{'}\right)$ determined by the major gas. Using equation (1), it is then straightforward to show that

$$\underline{\nabla} \cdot v^{'} = \frac{w^{'}}{H_s} - i\omega\frac{\rho_s^{'}}{\overline{\rho}_s} = \frac{w^{'}}{H_t} - i\omega\frac{\rho_t^{'}}{\overline{\rho}_t} \tag{9}$$

which leads to

$$\frac{\rho_s^{'}}{\overline{\rho}_s} = \frac{\rho_t^{'}}{\overline{\rho}_t} + \frac{iw^{'}}{\omega}\frac{(H_s - H_t)}{H_s H_t} \tag{10}$$

Equation (10) shows that the density fluctuations of the two species occur with a phase difference whose sign depends on the individual scale heights, H_s and H_t.

One can determine the collision frequency, ν_s, of a given s molecule with any t molecule using $\nu_s = K_{st}/\overline{\rho}_s$, where $\overline{\rho}_s = m_s\overline{n}_s$. A similar equation applies to ν_t with s and t interchanged everywhere. Altitude profiles of these collision frequencies are shown in Figure 1f. At low altitudes where the number density of N_2 exceeds

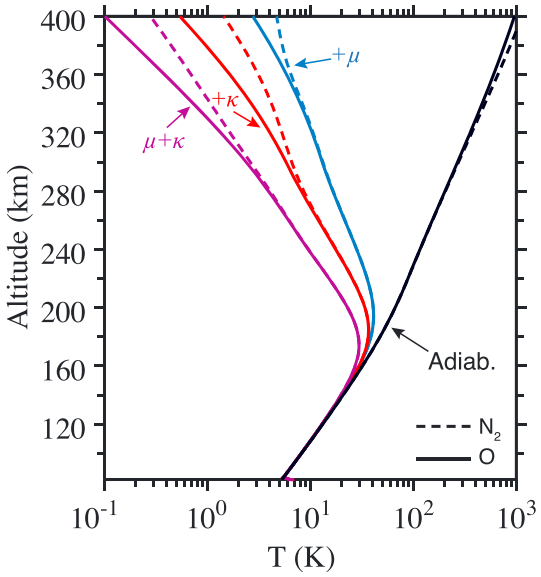

Figure 2. Effects of viscosity and thermal conductivity on wave temperature amplitudes for O and N_2 as a function of altitude for the isothermal case. The results are shown for viscosity acting alone (μ), thermal conductivity acting alone (κ), both of these acting together ($\mu + \kappa$), and for the adiabatic case.

that of O, the collision frequency of a single O atom with N_2 is significantly greater than the collision frequency of a single N_2 molecule with O. The collision frequencies decrease exponentially with increasing altitude for an isothermal atmosphere. The collision frequency for O in N_2 diminishes more rapidly than for N_2 in O because the former is proportional to the N_2 number density, while the latter is proportional to the O number density, and N_2 diminishes more rapidly with altitude than O.

In the following, we consider the effects of an upward propagating gravity wave with a period of 30 min and horizontal wavelength of 180 km. The wave has a phase speed of 100 m s^{-1}. These parameters are representative of waves observed by *Bertin et al.* [1978] and *Bertel et al.* [1978]. The phase speed is fast enough that vertical wavelengths are long enough to avoid strong scale-dependent dissipation low in the thermosphere and allow penetration of the wave into the region of the thermosphere where composition gradients are largest.

3. Results

3.1. Isothermal Atmosphere

The effects of viscosity and thermal conductivity on the amplitudes of the wave-induced temperature perturbations are shown as functions of altitude in Figure 2. The wave temperature amplitude grows with height in the absence of dissipation (the adiabatic case shown), and the temperature fluctuations are approximately equal at heights up to about 280–300 km. Beyond this height, collisions become infrequent enough to allow the gases to oscillate independently. With dissipation included, the wave temperature amplitude grows with height at low altitudes and peaks at about 180–200 km altitude. At higher altitudes, the wave temperature amplitude decreases with height due to effects of viscosity or thermal conductivity or both. Significant wave perturbations extend upward to 400 km altitude. N_2 and O temperature perturbations are essentially identical at altitudes below about 300 km. It is only above about 300 km altitude that the N_2 and O temperature perturbations become somewhat decoupled. Thermal conduction is more effective in limiting wave temperature amplitudes than is viscosity. This is explained by the fact that thermal conduction, which appears as a term in the heat equation, acts directly on the temperature perturbations, whereas the effects of viscosity on temperature perturbations enter indirectly, primarily through advective terms and velocity divergence. The smallest temperature amplitudes occur when viscosity and thermal conductivity act together, because in that case, the temperature perturbations and the velocity perturbations are simultaneously damped. At high altitudes, it is also seen that O experiences greater dissipation than N_2, which is due to the greater effective kinematic viscosity and effective thermal conductivity of O at these heights (see Figure 1d).

The effects of viscosity and thermal conductivity on wave temperatures are further elucidated by examination of the amplitude and phase of the ratio of the fractional O temperature perturbation (temperature perturbation divided by basic state temperature) to the fractional N_2 temperature perturbation (Figures 3b and 3f, respectively). In the adiabatic case, wherein viscosity and thermal conductivity are absent, relative fractional temperature amplitudes and phases are essentially the same below about 280 km altitude (by construction, they are identical at 120 km altitude and are maintained in thermal equilibrium in the collision-dominated region between about 120 km and 280 km), but above 280 km altitude, the amplitude of the fractional O temperature falls below that of the fractional N_2 temperature by as much as 30%. The relative fractional temperature ratio remains in

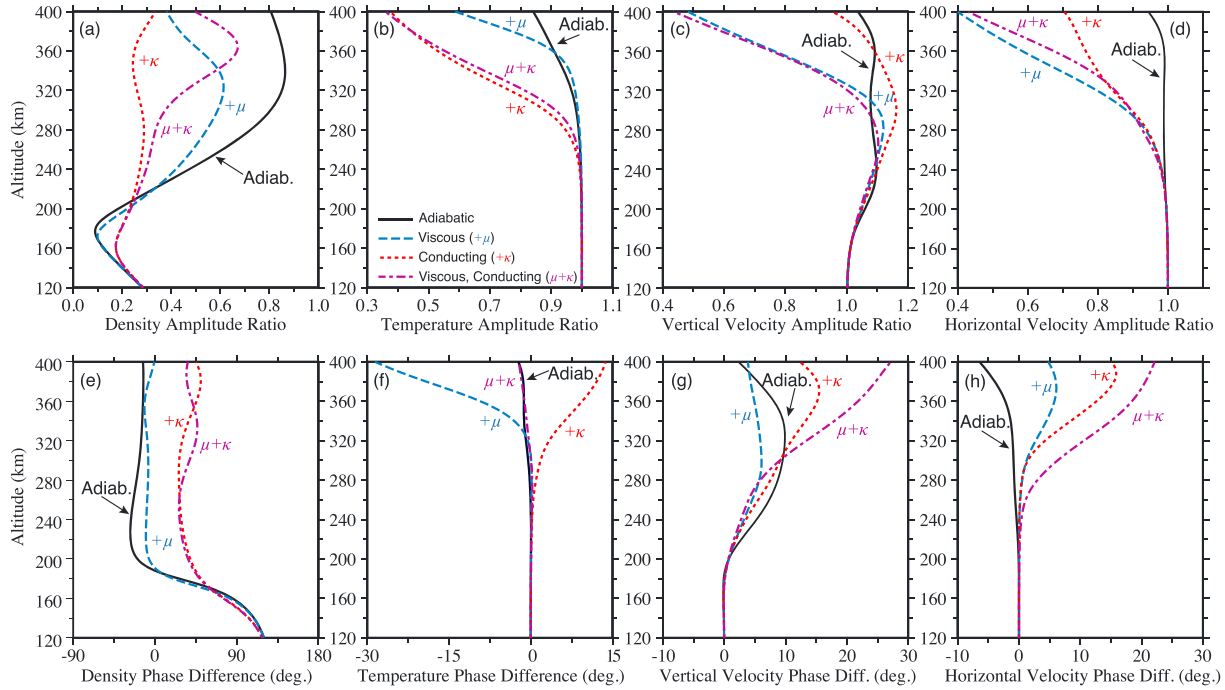

Figure 3. Altitude profiles of the amplitude of the ratio of (a) fractional density perturbation of O to that of N_2, (b) fractional temperature perturbation of O to that of N_2, (c) O vertical velocity perturbation to that of N_2, and (d) O horizontal velocity perturbation to that of N_2. (e–h) The corresponding phases are shown, respectively. The results are shown for the isothermal atmosphere.

phase until altitudes above about 400 km are reached (Figure 1f). When viscosity and thermal conductivity are considered, differences in fractional temperature perturbations between O and N_2 are even more profound. Thermal conductivity is more effective in establishing these differences than viscosity. When both thermal conductivity and viscosity are active, the amplitude of the fractional O temperature falls below that of the fractional N_2 temperature by as much as 75% at altitudes of about 400 km. Thermal conductivity and viscosity influence the phase of the relative fractional temperature ratio in opposite directions so that when both diffusivities are simultaneously considered, the fractional N_2 and O temperature perturbations are nearly in phase at all altitudes. As stated earlier, the effective kinematic viscosity and thermal conductivity for O is greater than it is for N_2, and so the O fluctuations experience greater dissipation than the N_2 fluctuations. *Del Genio et al.* [1979a, 1979b] concluded that temperature differences between species must be considered in order to accurately describe wave propagation characteristics above about 250 km altitude. Our study of the effects of thermal conductivity and viscosity reinforces and enhances this conclusion.

The amplitude and phase of the relative fractional density ratio between O and N_2 $\left(\left(\rho'/\bar{\rho}\right)_O/\left(\rho'/\bar{\rho}\right)_{N_2}\right)$ are shown in Figures 3a and 3e, respectively. In the adiabatic case, the amplitude of the ratio of the fractional O density to the fractional N_2 density decreases with height from 120 km to about 180 km and then increases with height reaching a value of about 0.85 at about 360 km altitude. The phase of this ratio varies widely at low altitudes approaching 0° at high altitude. The behavior of this ratio at low altitudes is in accord with the prediction of equation (10) and arises from the nonzero vertical velocity perturbation and the difference in the scale heights of the two species. Viscosity and thermal conductivity have relatively little effect on the ratio in the collision-dominated lower altitudes but strongly modify the ratio at high altitudes. Thermal conductivity alters the ratio more significantly than does viscosity. This is because density is directly relatable to temperature through the ideal gas law, and as we have discussed, temperature is more sensitive to thermal conduction than to viscosity. Note that the combined effects of viscosity and thermal conduction can have a smaller effect on the ratio than thermal condition or viscosity acting alone. This is a consequence of the ratioing and does not mean that the combined effects are less for each species individually. When both modes of dissipation are active, the amplitude of the ratio of the fractional O density to the fractional N_2 density is smaller than about 0.6 at all heights, and the phase of the ratio is nearly 45° at high altitudes.

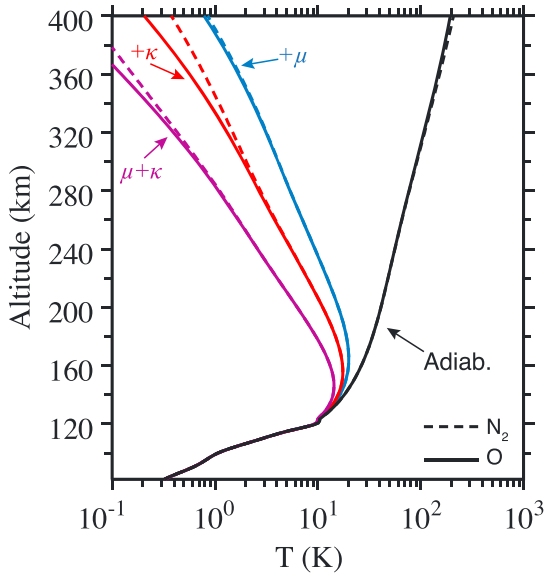

Figure 4. Effects of viscosity and thermal conductivity on wave temperature amplitudes for O and N_2 as a function of altitude for the nonisothermal case. The results are shown for viscosity acting alone (μ), thermal conductivity acting alone (κ), both of these acting together ($\mu + \kappa$), and for the adiabatic case.

Figures 3c and 3g show, respectively, the amplitude and phase of the ratio of the O vertical velocity perturbation to that of N_2. In the adiabatic case, the amplitude of the ratio stays approximately constant with height, and the phase of the ratio always lies close to 0°. However, with viscosity and thermal conductivity taken into account, above about 300 km altitude, the amplitude of the O vertical velocity falls significantly below that of the N_2 vertical velocity, and the phase difference between the vertical velocities grows significantly. Viscosity appears to play a dominant role in controlling the amplitude, while thermal conductivity appears to be more important in setting the phase.

The amplitude and phase of the ratio of the horizontal O velocity to the horizontal N_2 velocity are shown in Figures 3d and 3h, respectively. In the adiabatic case, the amplitude of this ratio is essentially 1 at all heights, while the phase is nearly 0° except for heights above about 360 km altitude when the phase can be as much as −15°. Viscosity and thermal conductivity change things dramatically; however, the amplitude of the ratio decreases with height above about 220 km reaching around 0.7 (when both viscosity and thermal conductivity are present), while the phase of the ratio increases from 0° at low altitudes to as much as 25° at high altitudes.

For the horizontal wind, viscosity alone has a much greater dissipative effect than thermal conduction alone. This is the opposite of what was found for temperature. The explanation for the stronger effect of viscosity is similar in nature to the explanation for the stronger effect of thermal conduction on temperature. It is explained by the fact that viscosity is a term in the momentum equation, and its effects are direct, whereas the effects of thermal conduction on the horizontal wind enter indirectly, mainly through the advective terms.

3.2. Nonisothermal Atmosphere

Results for the nonisothermal atmosphere corresponding to the isothermal results given in the previous section are shown in Figures 4 and 5. Comparison of Figures 4 and 2 shows that the main effect of nonisothermality is a reduction in temperature amplitude by about a factor of 2. Temperature amplitude peaks at a somewhat lower altitude in the nonisothermal case. The greater dissipation of the waves in the nonisothermal atmosphere is a direct consequence of the greater molecular kinematic viscosity and thermal conductivity below about 280 km altitude in the nonisothermal atmosphere (see Figures 1d and 1e).

Nonisothermality has only a small quantitative effect on the ratio of the fractional temperature perturbation of O to that of N_2 (compare Figures 5b and 3b and Figures 5f and 3f). The same can be concluded with regards to the ratio of the fractional O density to that of N_2 (Figures 5a and 3a and Figures 5e and 3e), the ratio of the O vertical velocity perturbation to that of N_2 (Figures 5c and 3c and Figures 5g and 3g), and the ratio of the O horizontal velocity perturbation to that of N_2 (Figures 5d and 3d and Figures 5h and 3h). At high altitudes, the N_2 fluctuation amplitudes are greater than the O fluctuation amplitudes because the effective kinematic viscosity and thermal conductivity are greater for O then for N_2 (see Figure 1d).

The differences seen in the results of the isothermal and nonisothermal cases are a direct consequence of the different mean number density distributions in the two cases. The N_2 (O) number densities are greater above ~240 km (270 km) altitude in the nonisothermal case (see Figure 1b). Consequently, collisional coupling between species is stronger (collisions are more frequent) at great heights in the nonisothermal atmosphere. Furthermore, below ~300 km altitude, the kinematic viscosity (Figure 1d) and the thermal diffusivity

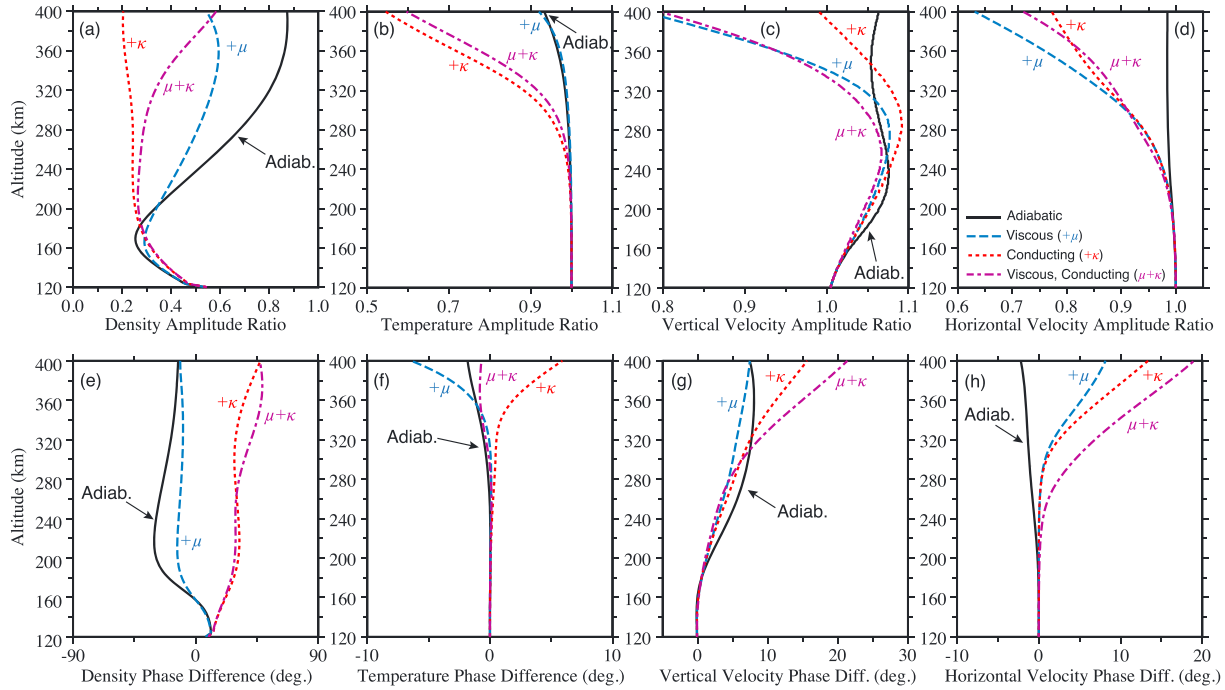

Figure 5. Altitude profiles of the amplitude of the ratio of (a) fractional density perturbation of O to that of N_2, (b) fractional temperature perturbation of O to that of N_2, (c) O vertical velocity perturbation to that of N_2, and (d) O horizontal velocity perturbation to that of N_2. (e–h) The corresponding phases are shown, respectively. The results are shown for the nonisothermal atmosphere.

(Figure 1e) are greater in the nonisothermal atmosphere. The net effect of these differences is that the waves are more strongly dissipated at lower thermospheric heights in the nonisothermal atmosphere (compare Figures 2 and 4). At greater heights in the nonisothermal case, the stronger collisional coupling between species causes the ratio of these fluctuations to vary more slowly with altitude compared to the isothermal case, as is evident in the adiabatic results shown in Figures 3b and 5b. Consequently, at greater heights in the nonisothermal atmosphere, the dissipation has less impact on the ratio of these fluctuations due to the stronger collisional coupling between the species, as seen by comparing Figures 3b and 5b.

4. Discussion

We have chosen a single wave with parameters similar to those that have been previously inferred from ground-based observations at *F* region heights by *Bertin et al.* [1978] and *Bertel et al.* [1978] and which were believed to have their sources in the lower atmosphere. These parameters are also similar to those of *Del Genio et al.* [1979b]. With a period of 30 min, a horizontal wavelength of 180 km, and a phase speed of 100 m/s, this wave has a large vertical wavelength and therefore avoids strong scale-dependent dissipation in the lower thermosphere. It is able to propagate to higher altitudes, where compositional effects are important. Other waves having different periods and phase speeds will be investigated in future studies.

Observations of multispecies fluctuations in the thermosphere can be made with in situ mass spectrometers, such as those that were carried aboard the AE-C and AE-E satellites [e.g., *Gross et al.*, 1984]. In these cases, large-scale waves were measured that were believed to be associated with geomagnetic substorms. A complication associated with such measurements is that the direction of wave propagation relative to the satellite could not be determined, and hence neither could the true horizontal wavelength. Hence, a comparison with previous experimental studies is limited. Very few measurements of individual species in the middle- and high-altitude thermosphere have been made since the mid-1970s, but these are needed in order to help clarify the dynamics of this region.

Based upon measurements acquired by a mass spectrometer on the Dynamics Explorer 2 satellite, *Innis and Conde* [2002, Table 1] have presented $\left(n'/\overline{n}\right)_O/\left(n'/\overline{n}\right)_{N_2}$ amplitudes and phases for a 15 min period, 400 km wavelength gravity wave near 350 km altitude. They have compared these ratios with those published by

Del Genio et al. [1979a] and found remarkably good agreement. Although the gravity wave parameters that we employ here are different from those discussed by *Innis and Conde* [2002], being 30 min and 180 km for the period and horizontal wavelength, respectively, it is nonetheless of interest for us to make a comparison with them. From Figures 5a and 5e, the amplitude and phase of $\left(n'/\overline{n}\right)_O/\left(n'/\overline{n}\right)_{N_2}$ based upon calculations that include both viscosity and thermal conductivity are approximately 0.40 and 45°, respectively. The corresponding values of *Innis and Conde* [2002] are 0.45 and 40°, respectively. This suggests a high degree of quantitative validity for our calculations, but in application, we would expect differences to exist associated with different wave periods, latitudes, level of solar activity, etc.

We have compared the results of some of our simulations for the isothermal basic state, excluding viscosity and thermal conductivity, with those shown in Figure 3 of *Del Genio et al.* [1979b]. The amplitude of our O/N_2 density ratio (Figure 3a) exhibits qualitative agreement with their results, increasing from small values (~0.1–0.2) near 175 km altitude to ~0.7–0.8 at higher altitudes. The phase of our O/N_2 density ratio (Figure 3e) is positive at low thermospheric heights, decreases with increasing altitude up to ~ −30° near 200 km altitude, and then slowly increases at greater heights while remaining slightly negative (~ −15°). Their phase starts from a negative value at 175 km altitude and increases with increasing height to a value of ~ 25° at greater heights. We have performed a number of simulations (not shown) that show that the phase is extremely sensitive to the wave period. *Del Genio et al.* [1979b] used a different mean state than we did, which would explain some of the differences.

Due to frequent N_2-O collisions at lower altitudes, these two species remain tightly coupled up to about 160 km altitude. Up to about 180 km altitude, N_2 is the dominant species, and through collisions, it controls the advection of O. The difference between the fractional fluctuation of density of N_2 and O is controlled by the difference in their respective scale heights and by the vertical velocity of N_2. Because the N_2 scale height is much smaller than the O scale height, O density perturbations are significantly smaller than the N_2 perturbations.

A few scale heights above 160 km, the species become decoupled, and the relative phases and amplitudes of N_2 and O are controlled by mutual diffusion, their differing scale heights and differing responses to viscosity and heat condition. The effects are both adiabatic and nonadiabatic. Adiabatic effects are mutual diffusion and differences in the exponential growth rate of individual species through the dependence of growth rate on scale height. The former effect (mutual diffusion) attempts to establish O to N_2 amplitude ratios near unity and relative phases near zero. The latter effect gives a more rapid increase with altitude for heavier species. Another adiabatic effect is the difference in vertical wave number caused by differences in static stability for individual species, again relatable to differences in individual scale heights. However, this last effect is not apt to be important unless one species is evanescent (or close to it) and the other is not. Thus, the adiabatic results show a tendency for ratios to approach unity as they become decoupled and then move toward lower values at high thermospheric altitudes. This is seen most clearly in the plots for relative density for the isothermal case (Figure 3a). For the nonisothermal atmosphere, differences in wave reflection from thermal gradients for individual species due to differences in the vertical wave numbers complicate the interpretation.

Nonadiabatic differences where the species decouple are due to differences in the effective viscosity and thermal conduction as a function of the relative abundance of the individual species [*Walterscheid and Hickey*, 2012]. As the dominance of O increases, the effect of thermal conduction and viscosity on N_2 becomes less, while the effects on O become greater. A secondary effect is the greater dissipation rate for the heavier species due to its smaller vertical wavelength. The net effect is to cause a large diminishment in the O to N_2 ratios relative to the adiabatic values and relative to unity at altitudes where the collisional coupling is weak.

5. Conclusions

Due to the strong collisional coupling between O and N_2, the velocity and temperature perturbations are affected in more or less the same way at low thermospheric altitudes. However, the density response of O relative to N_2 is significantly affected at low thermospheric altitudes by the differential advection of one species relative to the other with the result that the two species oscillate nearly in antiphase. At altitudes where the species become effectively decoupled, mutual diffusion causes the relative phase for the density

perturbations to rotate toward smaller values. The rotation is significantly less with viscosity and thermal conduction. The net effect of mutual diffusion, viscosity, and thermal conduction is to produce a relative phase near 45° with O leading N_2, while with mutual diffusion alone, it is generally slightly negative, with N_2 leading O.

This study demonstrates that viscosity and thermal conduction can significantly affect the oscillation of one species relative to another and can have large effects on the relative phases. These effects must be taken into account when interpreting data showing the variations of individual species in the diffusively separated region of the atmosphere.

Acknowledgments
M.P.H. was supported by NSF grant AGS-1001074 to Embry-Riddle Aeronautical University. R.L.W. and G.S. acknowledge support from NSF grants AGS1001086 and AGS-12455137. We thank J.B. Snively for his assistance in preparing the figures. We thank the referees for their comments. Copies of the simulation runs and figures can be obtained by emailing michael.hickey@erau.edu.

Michael Balikhin thanks Shin-ichiro Oyama and another reviewer for their assistance in evaluating this paper.

References

Bertel, L., F. Bertin, J. Testud, and D. Vidal-Madjar (1978), Evaluation of the vertical flux of energy into the thermosphere from medium scale gravity waves generated by the jet stream, *J. Atmos. Terr. Phys.*, *40*, 691.

Bertin, F., J. Testud, L. Kersley, and P. R. Rees (1978), The meteorological jet stream as a source of medium-scale gravity waves in the thermosphere: An experimental study, *J. Atmos. Terr. Phys.*, *40*(10–11), 1161–1183, doi:10.1016/0021-9169(78)90067-3.

Bruce, G. H., D. W. Peaceman, H. H. Rachford Jr., and J. D. Rice (1953), Calculations of unsteady state gas flow through porous media, *Petrol. Trans. AIME*, *198*, 79–92.

Burgers, J. M. (1969), *Flow Equations for Composite Gases*, Academic Press, New York.

Del Genio, A. D. (1978), Characteristics of acoustic gravity waves in a diffusively separated atmosphere, PhD, Univ. of California, Los Angeles.

Del Genio, A. D., J. M. Straus, and G. Schubert (1978), Effects of wave-induced diffusion on thermospheric acoustic-gravity waves, *Geophys. Res. Lett.*, *5*, 265–267, doi:10.1029/GL005i004p00265.

Del Genio, A. D., G. Schubert, and J. M. Straus (1979a), Characteristics of acoustic-gravity waves in a diffusively separated atmosphere, *J. Geophys. Res.*, *84*, 1865–1879, doi:10.1029/JA084iA05p01865.

Del Genio, A. D., G. Schubert, and J. M. Straus (1979b), Gravity wave propagation in a diffusively separated atmosphere with height-dependent collision frequencies, *J. Geophys. Res.*, *84*, 4371–4378, doi:10.1029/JA084iA08p04371.

Gross, S. H., C. A. Reber, and F. T. Huang (1984), Large-scale waves in the thermosphere observed by the AE-C satellite, *IEEE Trans. Geosci. Remote Sens.*, *22*, 340.

Hedin, A. E. (1991), Extension of the MSIS thermospheric model into the middle and lower atmosphere, *J. Geophys. Res.*, *96*, 1159–1172, doi:10.1029/90JA02125.

Hickey, M. P., and K. D. Cole (1987), A quartic dispersion equation for internal gravity waves in the thermosphere, *J. Atmos. Terr. Phys.*, *49*, 889–899.

Hickey, M. P., R. L. Walterscheid, M. J. Taylor, W. Ward, G. Schubert, Q. Zhou, F. Garcia, M. C. Kelly, and G. G. Shepherd (1997), Numerical simulations of gravity waves imaged over Arecibo during the 10-day January 1993 campaign, *J. Geophys. Res.*, *102*, 11,475–11,489, doi:10.1029/97JA00181.

Hickey, M. P., R. L. Walterscheid, and G. Schubert (2000), Gravity wave heating and cooling in Jupiter's thermosphere, *Icarus*, *148*, 266.

Innis, J. L., and M. Conde (2002), Characteristics of acoustic-gravity waves in the upper thermosphere using Dynamics Explorer 2 Wind and Temperature Spectrometer (WATS) and Neutral Atmosphere Composition Spectrometer (NACS) data, *J. Geophys. Res.*, *107*(A12), 1418, doi:10.1029/2002JA009370.

Lindzen, R. S., and H. L. Kuo (1969), A reliable method for the numerical integration of a large class of ordinary and partial differential equations, *Mon. Weather Rev.*, *97*, 732–734.

Schunk, R. W. (1977), Mathematical structure of transport equations for multispecies flows, *Rev. Geophys. Space Phys.*, *15*, 429.

Walterscheid, R. L., and M. P. Hickey (2012), Gravity wave propagation in a diffusively separated gas: Effects on the total gas, *J. Geophys. Res.*, *117*, A05303, doi:10.1029/2011JA017451.